Temperature Structure of Non-Flaring Loops

Nariaki Nitta

Lockheed Martin Solar and Astrophysics Laboratory
O/H1-12, B/252, 3251 Hanover Street, Palo Alto, CA 94304, U. S. A.
E-mail: nitta@lmsal.com

Abstract

The *Yohkoh* Soft X-ray Telescope (SXT) is a grazing incidence telescope. Temperature and emission measure maps can be obtained from the ratio of a pair of images in two filters that have different transmissions, assuming that each pixel or line of sight is dominated by plasma of a single temperature. Because of the broad temperature sensitivity of each filter, caution must be made when interpreting such filter ratio temperatures in the presence of plasmas of different temperatures along the line of sight. Here, we analyze SXT data in three filters in terms of two simple forms of differential emission measure (DEM), namely two delta functions and a single Gaussian. We also study how departure from the isothermal assumption affects the predicted radio brightness temperatures at 17 GHz, the primary frequency of the Nobeyama Radio Heliograph. Within the range of temperatures SXT can see, the effect is found to be quite small. Therefore, we need to assume the presence of much cooler ($T \ll 1$ MK) plasma, if the brightness temperature calculated from the SXT filter ratio temperature and emission measure is significantly higher than observed (c.f., Hanaoka 1999).

Key words: Sun: corona — Sun: X-rays, gamma rays — Sun: radio radiation

1. Introduction

Much of the solar corona is structured into hot ($\gtrsim$1 MK) closed loops as revealed in soft X-ray images. Although this has been known since the *Skylab* era, we still do not have a clear idea as to how these loops are heated. In order to forward our understanding of coronal heating, it is very important to obtain the temperature distribution in an isolated loop. Since the launch of *Yohkoh*, its Soft X-ray Telescope (SXT) has been the main provider of temperature maps. An SXT temperature map is obtained from the ratio of a pair of images in two filters that have different (and broad) transmissions. The underlying assumption of this so-called filter ratio method (e.g., Gerassimenko et al. 1978, Hara et al. 1992) is that plasma contained in a given pixel (or intersected by a given line of sight) has only one temperature.

This is probably an over-simplification, given that the solar corona is filled with loops of different temperatures, as revealed in groundbased observations of coronal emission lines (e.g., Ichimoto et al. 1995) as well as in extreme ultraviolet (EUV) images from other space borne experiments. Moreover, comparisons between X-ray and radio observations have often indicated the presence of plasma cooler than the temperature obtained from X-ray data (e.g., Strong et al. 1984, Nitta et al. 1991, Klimchuk and Gary 1995, Gary et al. 1996). In this report, we propose an alternative approach to analyze SXT data, allowing for distributions of temperatures along the line of sight, and apply it to the decay phase of a long duration event (LDE). Then radio brightness temperatures due to free-free emission are calculated using the parameters for the temperature distributions to better characterize the cooler plasma.

2. Broad-band Response of the SXT Instrument

We first recall that SXT is a grazing incidence telescope, and that the temperature response is quite broad. This is indicated in Figure 1, where the SXT temperature responses in the three most used filters (thin Aluminum, thick Aluminum and Beryllium) are plotted with similar information from other *Yohkoh* instruments; the temperature responses of the two lowest energy bands (L: 14–23 keV and M1: 23–33 keV) of the Hard X-ray Telescope (HXT) and the contribution functions of the resonance lines observed by the Bragg Crystal Spectrometer (BCS).

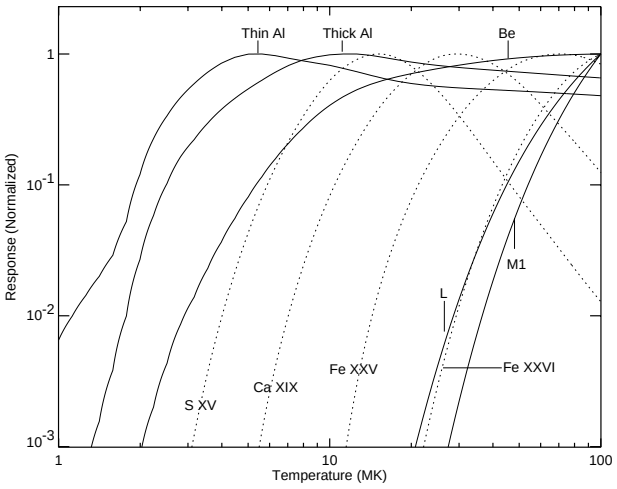

Fig. 1.. Response of SXT and HXT with temperature (solid lines). The curves for three filters (Thin, Thick and Be) of SXT and two channels (L and M1) of HXT are drawn. Dotted lines show contribution functions of the resonance lines of 4 ions that are observed with BCS. The curves for Be, L, M1 and Fe XXVI are normalized at 100 MK.

In the early part of flares, the SXT filter ratio temperature, even with the two thickest filters (thick Al and Be), is almost invariably lower than the temperature derived from the BCS Fe XXV channel (typically 20–25 MK). This is due to the presence of cool ($T \lesssim$10 MK) plasma that is observed by SXT but not by BCS (Nitta and Yaji 1997). The presence of plasma cooler than the filter ratio temperature automatically implies the presence of hotter plasma, meaning the distribution of temperatures along the line of sight. This distribution also causes different filter ratios to yield different temperatures, as observed in non-flaring loops as well as flares (Nitta, Yaji 1997). Therefore, even though a single filter ratio temperature can be a good indicator of plasma temperature, its blind use can be misleading, especially for quantitative modelling. We argue that a single filter ratio temperature should give way to analysis allowing for multi-thermal plasmas, i.e., differential emission measure (DEM) analysis.

3. DEM Models and Radio Brightness Temperature

Until quite recently, SXT large-scale (partial frame) images had routinely been taken in two filters for non-flare periods, i.e., only one filter ratio was available. This was to avoid losing reasonable time resolution, but is part of the reason for the rareness of DEM analysis on SXT data. In contrast, the flare sequence data have almost always included all the three filters indicated in Figure 1. The flare sequence data occasionally extend to the decay phase of a long duration event (LDE), during which the filter ratio temperature decreases to typical values of an active region loop outside flare periods.

Here we apply two simple DEM models to SXT data in the three filters. The first model consists of two delta functions in temperature. This DEM has four parameters, T and EM of hotter (H) and cooler (C) plasmas, one of which has to be given, because only three measurements are available. We arbitrarily fix T_C to be either 3.0 MK or 5.5 MK. Another DEM is a single Gaussian of the form $EM_0 \cdot \exp(-(T - T_0)^2/\sigma_T^2)$, with three parameters T_0, σ_T and EM_0.

Instead of studying the temperature maps in detail, we discuss the DEM of the typical pixels in two selected areas of the long duration event (LDE) that took place on 15/16 March 1993. This event was described by Hanaoka (1999) as posing difficulty in terms of reconciling observed and calculated radio brightness temperatures. The loop top is more pronounced in SXT images compared with the footpoints, and as a result, the radio brightness temperature at the loop top is considerably higher than observed. Three-filter SXT data are available only during the early part of the decay phase, some 100 minutes before the period analyzed by Hanaoka (1999).

In Table 1, we summarize the calculated parameters of the above DEM models for the loop top and northern footpoint sources, in addition to the single filter ratio temperatures and emission measures. These parameters reproduce the observed count in each filter to an accuracy of 0.1 %. In the table, we note that the hotter component

Table 1. Summary of the plasma parameters of the LDE of 15/16 March 1993

	Loop top	Northern footpoint
T (MK), EM (10^{29} cm^{-5}) from thick Al/thin Al	6.84, 41.1	5.92, 10.3
T (MK), EM (10^{29} cm^{-5}) from Be/thick Al	8.38, 35.4	6.74, 8.75
T_H, EM_H EM_C for T_C=3.0 MK	9.3, 28.4, 27.0	8.1, 5.56, 9.52
T_H, EM_H EM_C for T_C=5.5 MK	10.8, 17.4, 24.9	12.2, 1.26, 9.19
T_0, σ_T, EM_0	6.84, 1.83, 96.7	5.11, 1.82, 26.8

of the two-temperature models has higher temperatures than either of the two filter-ratio temperatures. It actually approaches T(Be/thick Al), as T_C is set to be smaller. For larger values of T_C, T_H becomes larger but EM_H does not decrease dramatically. For example, we have T_H=80 MK and EM_H=3.35×10^{29} cm^{-5} for T_C=6.70 MK at the loop top, which would produce enough counts to be observed in the HXT M1 band, contrary to the observation. In the Gaussian DEM, $T_0 \lesssim T$(thick Al/thin Al).

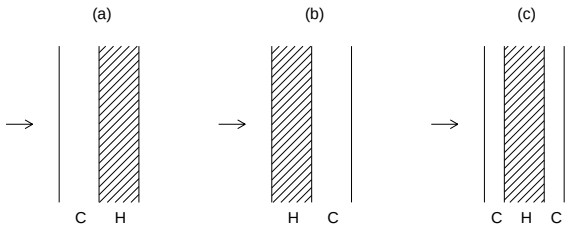

Fig. 2.. Simple distributions of two-temperature plasma with respect to the observer (to the left as indicated by arrows).

Next we calculate the brightness temperature at 17 GHz from the parameters shown in Table 1. The opacity due to thermal bremsstrahlung (free-free) is given by

$$\tau = 9.8 \times 10^{-3}(\nu \pm \nu_c \cos\alpha)^{-2} \times T^{-1.5} \ln\left(\frac{4.7 \times 10^{10} T}{\nu}\right) \int n_e^2 dl, \quad (1)$$

where T is the plasma temperature; ν is the observing frequency; n_e is the density; $\int n_e^2 dl$ is the column emission measure; ν_c is the cyclotron frequency ($\nu_{c,\mathrm{MHz}} = 2.8 B_G$); and α is the angle between the magnetic field and the line of sight (Zheleznyakov 1970). Here we neglect $\nu_c \cos\alpha$ because the effect is small, consistent with the lack of observed polarization associated with the loop top source in LDEs (Hanaoka 1999). The brightness temperature from this isothermal plasma is

$$T_B = T(1 - e^{-\tau}). \quad (2)$$

If the line of sight intersects n layers of distinct temperatures, the brightness temperature will depend on how they are geometrically distributed with respect the line of sight (c.f., Vourlidas and Bastian 1996). For example, even if the plasma along the line of sight is characterized by two temperatures, we can consider various cases of their distributions (see Figure 2). They possibly lead to different values of the brightness temperature, which is the summation of contributions from the individual layers (a total of n) attenuated by layers in the foreground, i.e.,

$$T_B = \sum_{i=1}^{n} T_i (1 - e^{-\tau_i}) \exp\left(-\sum_{j<i} \tau_j\right). \quad (3)$$

In Table 2, we compare the calculated brightness temperatures at 17 GHz from the parameters of the two single filter ratios and the two forms of DEM. It is found that the effect of varied geometrical distributions (Figure 2) is quite small, especially for the Gaussian DEM. The range inserted for the two-temperature cases corresponds to Figures 2(a) and 2(b), respectively, which present the minimum and maximum. Apart from the ratio Be/Thick Al,

Table 2. Calculated brightness temperature (MK) at 17 GHz due to the parameters of Table 1.

	Loop top	Northern footpoint
thick Al/thin Al	0.84	0.23
Be/thick Al	0.67	0.19
Two-temperature: T_C=3.0 MK	1.13 – 1.22	0.38 – 0.39
Two-temperature: T_C=5.5 MK	0.84 – 0.85	0.24 – 0.24
Gaussian	0.90	0.30

which ignores contributions of cool plasma observed primarily in the thin Al filter and so is unrealistic, the brightness temperature calculated from the Thick Al/Thin Al is the lowest. The two forms of DEM do not contribute to lower the calculated brightness temperature.

4. Concluding Remarks

We have proposed a new approach for analyzing SXT data, in which the likely presence of more than one temperature along the line of sight is taken into account. Because SXT has only a few X-ray filters, we are limited to simple forms of DEM.

The radio brightness temperature (due to free-free emission) has been calculated for temperatures and emission measures obtained from SXT in different ways. But the inclusion of DEM does not seem to help us solve the problem of Hanaoka (1999), namely that the calculated brightness temperature at 17 GHz is ∼50 % higher than observed. Although our interval is different from Hanaoka's, our result indicates that, within the sensitivity range of SXT, the parameters from the single filter ratio Thin Al/Thick Al leads to the lowest calculated brightness temperature at 17 GHz. Therefore, we attribute the lower observed brightness temperature to the presence of plasma cooler than SXT can see. Work is under way to confirm this with the joint datasets of soft X-ray, EUV and radio images.

This work was supported by NASA grant NAS 8-40801.

References

Gary G.E. et al. 1996, ApJ 464, 965
Gerassimenko M., Nolte J.T. and Solodyna C.V. 1978, Sol Phys. 57, 103
Hanaoka Y. 1999, in these proceedings
Hara H. et al. 1992, PASJ, 44, L135
Ichimoto, K. et al. 1995, ApJ, 445, 978
Klimchuk J.A. and Gary D.E. 1995, ApJ 448, 925
Nitta N. et al. 1991, ApJ 374, 374
Nitta N. and Yaji K. 1997, ApJ 484, 927
Strong K.T., Alissandrakis C.E. and Kundu M.R. 1984, ApJ 277, 865
Vourlidas A. and Bastian T.S. 1996, ApJ 466, 1-39
Zheleznyakov V.V. 1970, Radio Emission of the Sun and Planets (Pergamon, Oxford)